EFFECTS OF ENVIRONMENT ON THE SURFACE WAVE CHARACTERISTICS OF A DIELECTRIC-COATED CONDUCTOR

PART II

(MISS) GLORY JOHN, (MRS.) R. CHATTERJEE AND S. K. CHATTERJEE

(*Electrical Communication Engineering, Indian Institute of Science, Bangalore 560012*)

Received on November 22, 1974

ABSTRACT

Theoretical investigation on the surface wave characteristics of a lossless, dielectric-coated conductor embedded in an infinitely extended lossless anisotropic dielectric medium show that as the ratio of the axial dielectric constant (ϵz) *to the radial dielectric constant* ($\epsilon \rho$) *is increased, the surface wave tends to become more strongly bound.*

1. INTRODUCTION

It has been reported [1] recently that a cylindrical conductor coated with a lossless dielectric and immersed in an infinitely extended lossless dielectric medium and excited by Eo-wave can support surface wave as long as the dielectric constant of the outside medium remains less than the dielectric constant of the inside dielectric medium. The authors have also shown [2] that the surface wave solution of a lossy dielectric-coated conductor immersed in a lossy dielectric medium and excited in Eo-mode breaks down under certain condition. It may then be said that the surface wave energy is transformed into radiated energy under the condition when surface wave is no more supported.

The propagation of plane electromagnetic waves in regions with anisotropic permittivity or permeability has received considerable attention in the literature—the former in connection with the study of the optical properties of crystals [3] and the electromagnetic behaviour of the ionosphere [4, 5] and the latter in connection with magnetised ferrites [6]. The excitation of unidirectional plane surface waves on a perfectly conducting screen covered with an anisotropic plasma sheath has also been treated [7]. Theoretical analysis of the propagation characteristics of microwaves through waveguides whose walls are anisotropic has also been reported [8, 9, 10].

There seems to be no available information on the surface wave characteristics of a dielectric-coated conductor immersed in an anisotropic dielectric medium. The present report is also concerned with the theoretical analysis of the surface wave characteristics of a dielectric-coated conductor surrounded by an infinitely extended lossless anisotropic dielectric medium. The effect of variation of the anisotropicity of dielectric constant of the outside medium on the radial propagation constant, guide wavelength, constant percentage power contour, phase velocity of the surface wave and the percentage of power flow in the outside medium, etc., has been studied in detail. The results lead to some interesting conclusions in contrast with the isotropic case dealt with in Part I.

2. FORMULATION OF THE PROBLEM

As shown in Fig. 1, the structure under consideration is a circular cylindrical conductor (Med. I, $\sigma = \infty$) coated with a lossless isotropic dielectric of dielectric constant ϵ_1 (Med. II, $\sigma = 0$, $\mu = \mu_0$) surrounded by an infinitely extended lossless dielectric of tensor dielectric constant $\underset{\sim}{\epsilon}$ (Med. III, $\sigma = 0$, $\mu = \mu_0$) which is anisotropic having components ϵ_ρ and ϵ_z where z is the direction of propagation and ρ is the transverse radial coordinate and $\epsilon_\rho = \epsilon_z$ when the dielectric is a scalar. The dielectric tensor $\underset{\sim}{\epsilon}$ in medium III is given by the relation

$$\underset{\sim}{\epsilon} = \begin{pmatrix} \epsilon_\rho & 0 & 0 \\ 0 & \epsilon_\rho & 0 \\ 0 & 0 & \epsilon_z \end{pmatrix} \tag{1}$$

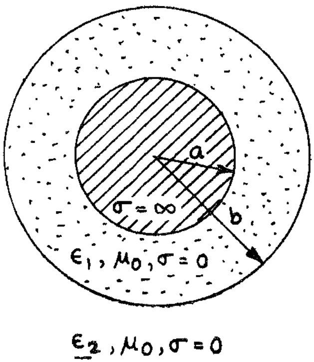

FIG. 1. Dielectric-coated conductor embedded in anisotropic dielectric medium.

The permeability μ in all the three media is equal to the free space permeability μ_0 and the conductivity in the first medium is $\sigma = \infty$, but in the other two media $\sigma = 0$.

The wave equations in the I, II and III media are,

$$\frac{\partial^2 E_z}{\partial \rho^2} + \frac{1}{\rho}\frac{\partial E_z}{\partial \rho} + \frac{\partial^2 E_z}{\partial z^2} + j\omega\mu_0\sigma E_z = 0 \tag{2}$$

$$\frac{\partial^2 E_z}{\partial \rho^2} + \frac{1}{\rho}\frac{\partial E_z}{\partial \rho} + \frac{\partial^2 E_z}{\partial z^2} + \omega^2 \mu_0 \epsilon_1 E_z = 0 \tag{3}$$

and

$$\frac{\partial^2 E_z}{\partial \rho^2} + \frac{1}{\rho}\frac{\partial E_z}{\partial \rho} + \left(\frac{E_z}{\epsilon_\rho}\right)\frac{\partial^2 E_z}{\partial z^2} + \omega^2 \mu_0 \epsilon_z = 0. \tag{4}$$

3. Field Components

The field components obtained by solving the first two wave equations (2 and 3) in media I ($0 c\rho c a$) and II ($a \leq \rho \leq b$) are the same as reported in Part I [1] of this paper. The field components obtained by solving equation (4) for the third medium and using Maxwell's equations are

Medium III $\rho \geqslant b$

$$E_{z3} = DH_0^{(1)}(ju_0\rho)\, e^{j\omega t - \gamma z}$$

$$E_{\rho 3} = -j\frac{\gamma\epsilon_z}{u_2\epsilon_\rho} DH_1^{(1)}(ju_2\rho)\, e^{j\omega t-\gamma z}$$

$$H\phi_3 = \frac{k_2^2}{\omega\mu_0 u_2}\left(\frac{\epsilon_z}{\epsilon_\rho}\right) DH_1^{(1)}(ju_2\rho)\, e^{j\omega t-\gamma z} \tag{5}$$

where

$$u_2^2 = -\left[\frac{\epsilon_z}{\epsilon_\rho}\gamma^2 + k_0^2\,\epsilon_z\right]$$

$$k_2^2 = k_0^2\,\epsilon_\rho \tag{5 a}$$

Since $u_1^2 = k_1^2 + \gamma^2$, the radial propagation constants u_1 in the second medium and u_2 in the third medium are related by the relation

$$u_1^2 + \frac{\epsilon_\rho}{\epsilon_z} u_2^2 = k_1^2 - k_0^2\epsilon_\rho \tag{6}$$

i.e.,

$$u_1^2 = k_0^2(\epsilon_1 - \epsilon_\rho) - u_2^2/s \tag{6 a}$$

where

$$s = \frac{\epsilon_z}{\epsilon_\rho}$$

4. CHARACTERISTIC EQUATION

Due to the vanishing of the ϵ_{z_2} at $\rho = a$ in the second medium, the relation between the excitation constants B and C is [1]

$$\frac{C}{B} = -\frac{J_0(u_1a)}{Y_0(u_1a)} \tag{7}$$

The excitation constants C and B are involved in the field components in the second medium. Expressing the field components in the second medium in terms of one excitation constant B or C and matching the wave impedances at $\rho = b$,

$$\left.\frac{E_{z2}}{H\phi_2}\right|_{\rho=b} = \left.\frac{E_{z3}}{H\phi_3}\right|_{\rho=b} \tag{8}$$

the following characteristic equation is obtained:

$$\frac{\epsilon_1}{\epsilon_z}\frac{u_2}{u_1}\cdot\frac{K_0(u_2b)}{K_1(u_2b)} + \frac{J_0(u_1b)\,Y_0(u_1a) - J_0(u_1a)\,Y_0(u_1b)}{J_1(u_1b)\,Y_0(u_1a) - J_0(u_1a)\,Y_1(u_1b)} \tag{9}$$

The equations (6 *a*) and (9) are solved to yield u_1 and u_2 as functions of the different physical parameters of the structure. The other propagation characteristics such as the axial propagation constant γ, the phase constant β, the guide wavelength λ_g and the phase velocity v_ρ obtained from the following relations are related to the radial propagation constants

$$\gamma = j\beta = j\sqrt{u_2^2/s + k_0^2\epsilon_{\rho\gamma}}$$

$$\beta = \sqrt{u_2^2/s + k_0^2\,\epsilon_\rho}$$

$$\lambda_g = 2\pi/\beta$$

$$v_\rho = \omega/\beta \tag{10}$$

are evaluated with respect to different physical parameters and are presented graphically in Figs. 2–6.

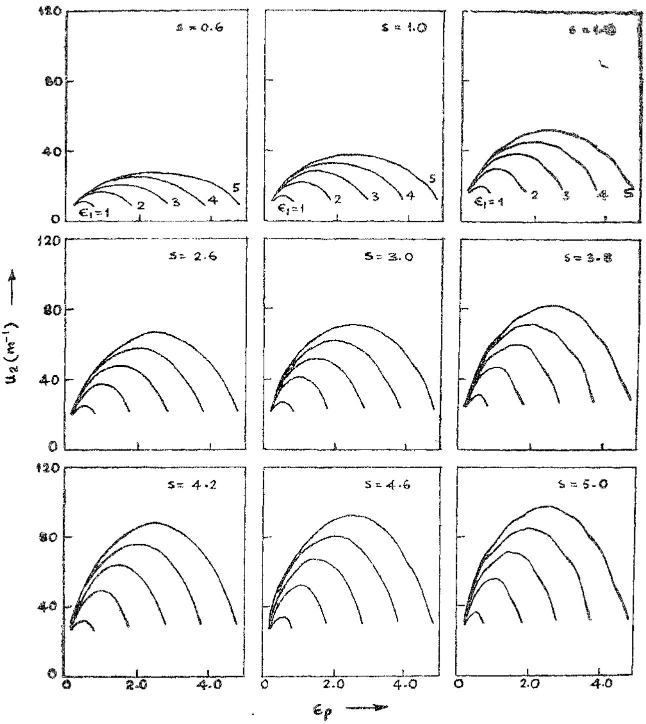

FIG. 2. Variation of U_2 with ϵ_p. $a = 0 \cdot 001$ m; $b = 0 \cdot 0011$ m.

The radial field decay for the components E_z and E_ρ in the third medium is plotted as a function of s in Fig. 7 by using equations (5) and (5 a).

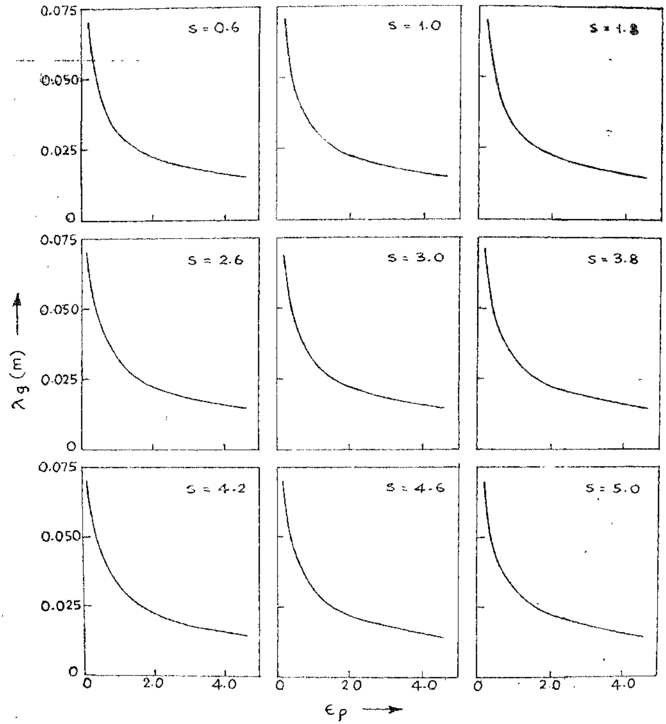

Fig. 3. Variation of λ_g with ϵ_ρ. $a = 0{\cdot}001$ m; $b = 0{\cdot}0013$ m.

5. Power Flow

The power flow along the z-direction in medium II and medium III are given respectively by the following relations:

$$\rho_{z2} = \tfrac{1}{2}\, Re \int_{\phi=0}^{2\pi} \int_{\rho=a}^{b} E\rho_2 H_{\phi_2}{}^{*} \rho d\rho d\phi$$

$$= \frac{\pi\omega\beta\epsilon_1}{2u_1{}^2\, Y_0{}^2(u_1 a)}\, BB^{*} \left\{\rho^2 \left[Y_0{}^2(u_1 a) \left\{ J_0{}^2(u_1\rho) \right.\right.\right.$$

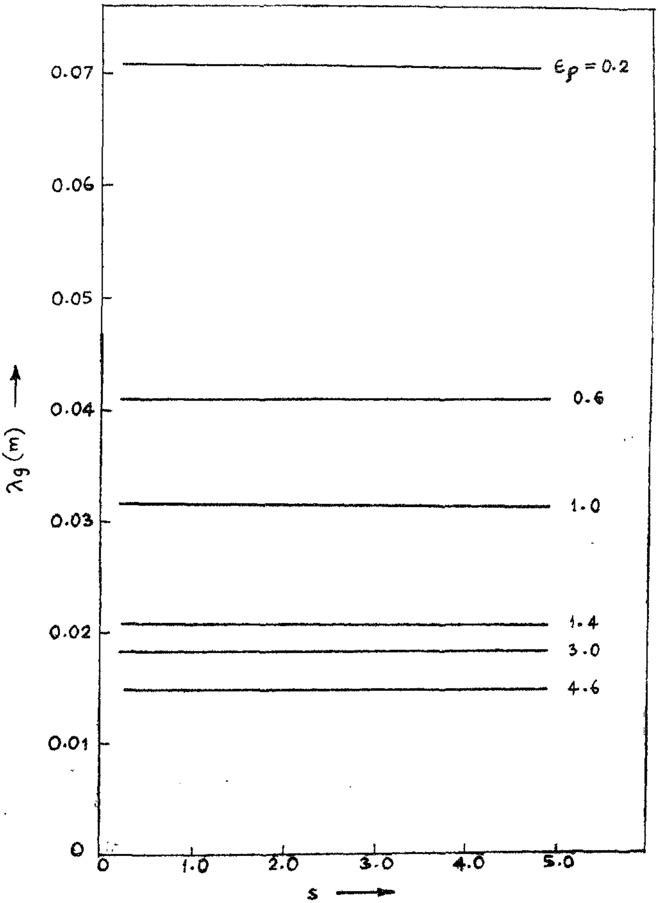

Fig. 4. Variation of λ_g with s. $a = 0{\cdot}001$ m; $b = 0{\cdot}0011$ m.

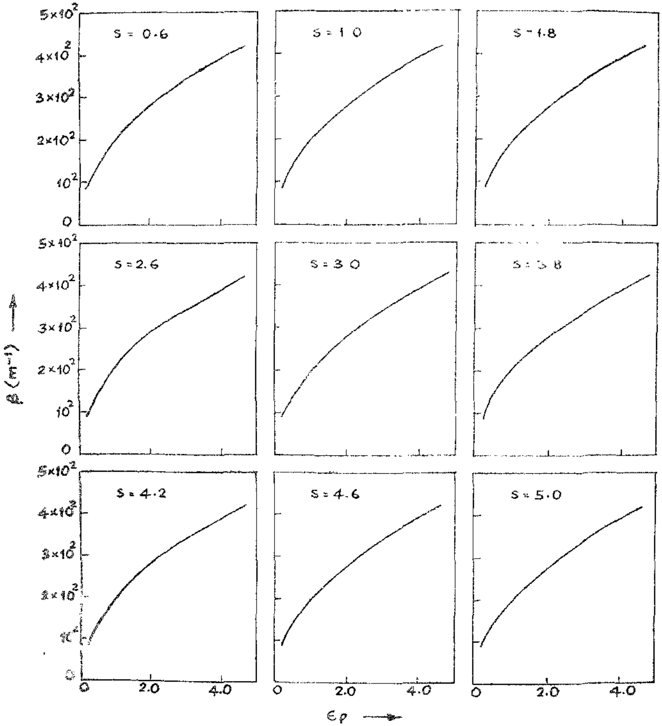

FIG. 5. Variation of β with ϵ_ρ. $a = 0{\cdot}001\ m$; $b = 0{\cdot}0013\ m$.

$$+ J_1^2(u_1\rho) - \frac{2}{u_1\rho} J_0(u_1\rho) J_1(u_1\rho) \Big\} + J_0^2(u_1 a)$$

$$\times \Big\{ Y_0^2(u_1\rho) + Y_1^2(u_1\rho) - \frac{2}{u_1\rho} Y_0(u_1\rho) Y_1(u_1\rho) \Big\}$$

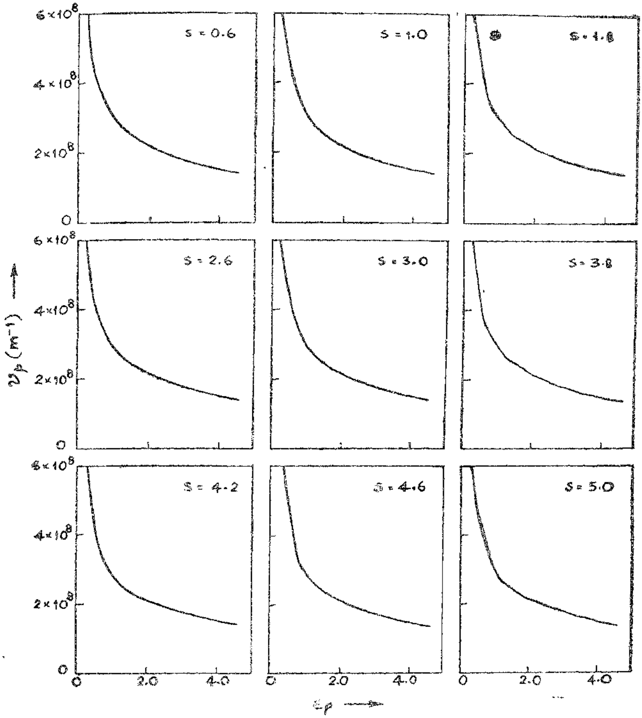

FIG. 6. Variation of v_φ with ϵ_ρ. $a = 0{\cdot}001$ m; $b = 0{\cdot}0013$ m.

$$+ 2J_0(u_1a)\,Y_0(u_1a)\Big[J_0(u_1\rho)\,Y_0(u_1\rho) + J_1(u_1\rho)\,Y_1(u_1\rho)$$

$$- \frac{1}{u_1\rho}\{J_0(u_1\rho)\,Y_1(u_1\rho) + J_1(u_1\rho)\,Y_0(u_1\rho)\}\Big]\Big]_{\rho=a}^{\rho=\infty}\Bigg\} \qquad (11)$$

$$P_{z_3} = \tfrac{1}{2}\,Re \int_{\phi=0}^{2\pi}\int_{\rho=b}^{\infty} E\rho_3 H\phi_3{}^* \rho\, d\rho\, d\phi$$

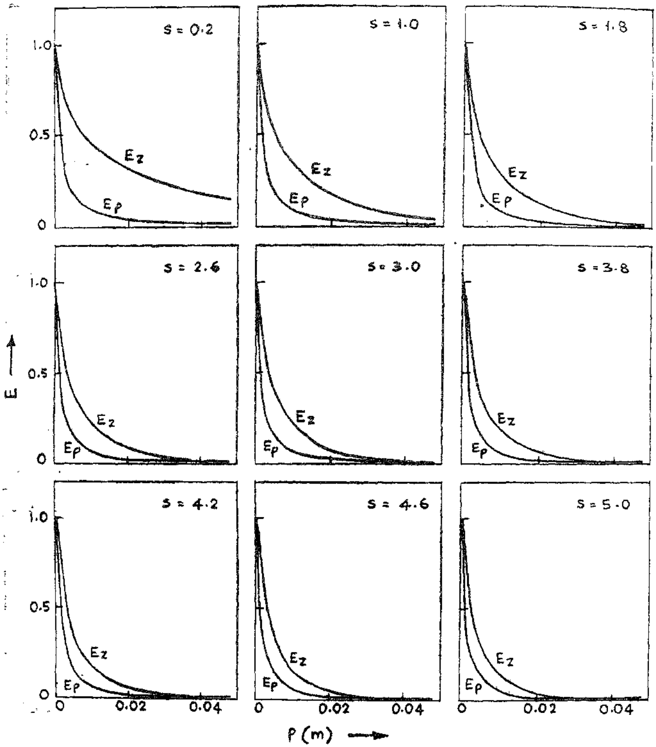

FIG. 7. Variation of E_z and E_ρ with ρ. $a = 0 \cdot 001$ m; $b = 0 \cdot 001$ m; $\epsilon_\rho = 2 \cdot 6$; $\epsilon_z = 5 \cdot 0$.

$$= DD^* \frac{2\omega\beta\epsilon_0\epsilon_z s b^2}{\pi u_2^2}\Big[K_0^2(u_2 b) - K_1^2(u_2 b) + \frac{2}{u_2 b} K_0(u_2 b)\, K_1(u_2 b)\Big] \tag{12}$$

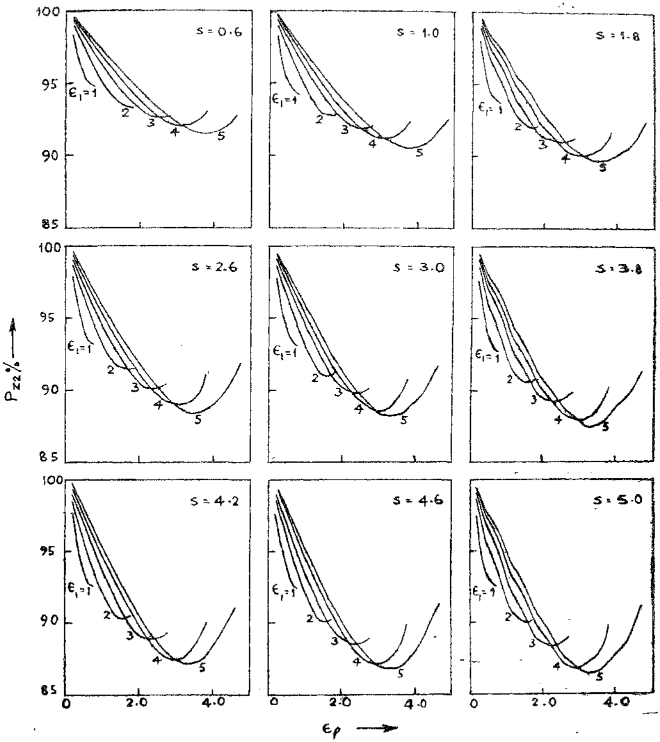

FIG. 8. Variation of pz_3 with ϵ_ρ. $a =$ 0·001 m; $b =$ 0·0013 m.

The constant percentage power contours are calculated from the following relation:

$$p = 1 - \frac{\rho_p^2}{b^2} \frac{F(u_2\rho_p)}{F(u_2b)} \tag{13}$$

where p represents a certain percentage of the total power within a circle of radius ρ_p and

$$F(u_2\rho) = K_0^2(u_2\rho) - K_1^2(u_2\rho) + \frac{2}{u_2\rho} K_0(u_2\rho) K_1(u_2\rho), \quad \rho = \rho_p, b \tag{14}$$

Figurs 8 shows the percentage of the total power flow outside the structurein the z-direction as function of ϵ_p, s and ϵ_1.

Figure 9 shows the constant percentage power contour as function of ϵ_p, s and ϵ_1.

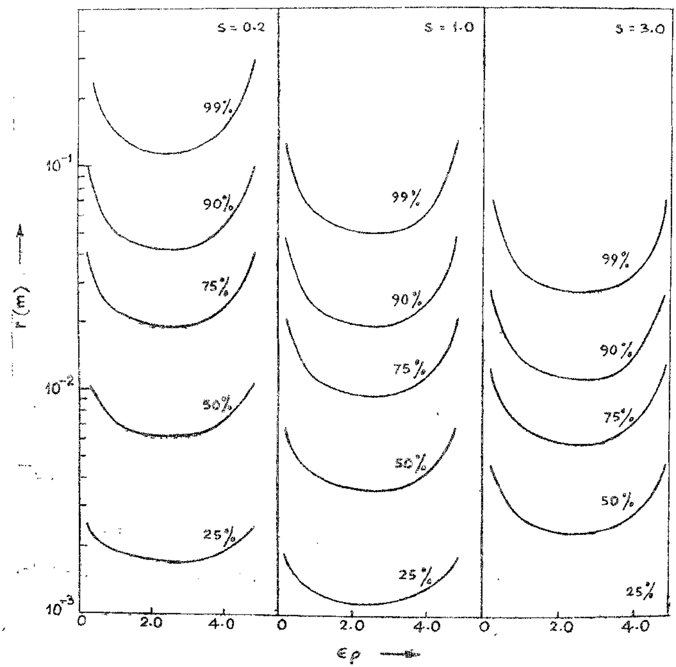

FIG. 9. Variation of percentage power contour with ϵ_p. $a = 0{\cdot}001$ m; $b = 0{\cdot}0011$ m

6. Conculsions

The following conclusions regarding the effects of anisotropicity of the third medium on the surface wave characteristics of the structure can be drawn.

(i) The degree (s) of anisotropicity influences appreciably the value of the radial propagation constant and hence the radial field decay (*see* Figs. 2 and 7). An increase in the value of s increases u_2 which results in a faster decay of the electric field in the third medium leading to a more strongly bound surface wave. This is also evident from the β, λ_g and V_p curves (*see* Figs. 4–6).

(ii) The radius of the constant percentage power contour shrinks with increase in the value of s (Fig. 9). Percentage of total power flow in the 3rd medium also decreases with increase in the value of s (Fig. 8). Both these results also support the previous conclusion.

(iii) It is thus possible to concentrate more energy in the second medium by controlling the anisotropy factor (s) and if the second medium is negligibly lossy, as has been assumed, it is possible to transmit microwave power to a longer distance than the isotropic case.

7. References

[1] Glory John and Chatterjee, S. K. .. Effects of environment on the surface wave characteristics of a dielectric-coated conductor—Part I. *Jour. Ind. Inst. Sci.*, 1974, 56, 88–103.

[2] Glory John, Chatterjee, R. (Mrs.) and Chatterjee, S. K. Surface wave characteristics of a lossy dielectric-coated conductor immersed in a lossy dielectric medium. *Proc. I.E.RE. (India)* (To be published).

[3] Born, M. and Wolf, E... *Principles of Optics*, Ch. XIV, Pergamon Press, 1959.

[4] Ratcliffe, J. A. .. *The Magneto-Ionic Theory and Its Application to the Ionosphere*, Cambridge University Press, 1960.

[5] Budden, K. G. .. *Radio Waves in the Ionosphere*, Cambridge University Press, 1961.

[6] Clarricoats, P. J. B. .. *Microwave Ferrites*, Wiley, 1961.

[7] Seshadri, S. R. .. Surface waves on an anisotropic plasma sheath, *IRE-Trans.*, 1964, MTT-12, 529–541.

[8] Karbowiak, A. E. .. Microwave propagation in anisotropic waveguides. *Proc. IEE* Part C, 1956, 103, Pp. 139–144.

[9] Unger, H. G. .. *Waveguides with Anisotropic Impedance Walls*, *Electromagnetic Waves*, Part II, Edited by E. C. Jordan, Pergamon Press 1963, pp, 919–939.

[10] Chang, C. J. M. . Circular waveguides lined with artificial anisotropic dielectrics *IRE-Trans.*, 1972, *MTT*-20, 517–523.